Investigation of the Seismic Behavior of Brace Frames with New Corrugated All-Steel Buckling Restrained Brace

Mehdi Ebadi Jamkhaneh, Amir Homaioon Ebrahimi & Maedeh Shokri Amiri

International Journal of Steel Structures

ISSN 1598-2351

Int J Steel Struct
DOI 10.1007/s13296-018-00202-2

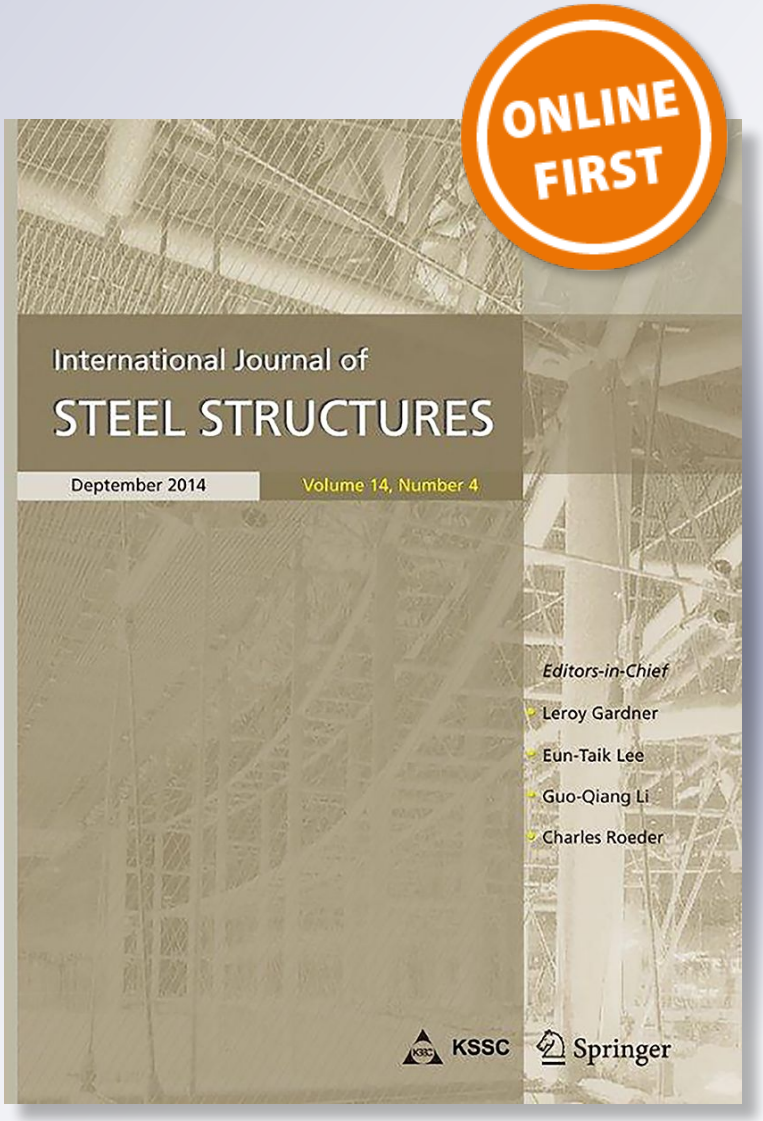

Springer

International Journal of Steel Structures
https://doi.org/10.1007/s13296-018-00202-2

Online ISSN 2093-6311
Print ISSN 1598-2351

Investigation of the Seismic Behavior of Brace Frames with New Corrugated All-Steel Buckling Restrained Brace

Mehdi Ebadi Jamkhaneh[1] · **Amir Homaioon Ebrahimi**[2] · **Maedeh Shokri Amiri**[3]

Received: 20 September 2018 / Accepted: 27 December 2018

Abstract
All-steel buckling restrained brace (BRB) is a type of relatively new common bracings considering its low weight and whilst it is not required curing of mortar at the core of braces. In this study, a new form of all-steel BRB is introduced with corrugated edges of the core and the external sheath, and it was analyzed by using of finite element method. Existence of corrugated and ribbed edges led to enhance of buckling resistance. Numerical model was validated with laboratory samples, and after receiving an acceptable compliance in model behavior, the numerical models were offered. In this analysis, key parameters were size of brace section and distance of gap between the internal and external sheaths. The most appropriate size for gap between the core and external tube was determined to be 10 mm. Upon specifying the non-linear modeling parameter, two cases of frame with ordinary concentrically brace and the proposed all-steel BRB were compared for three structures with 4, 8 and 12 floors using pushover and non-linear time history analysis. The results demonstrated that utilizing of the proposed BRB will lead to an increase in behavior coefficient and structure ductility as well as an alteration in performance level of tall structures from collapse prevention to life safety level.

Keywords All-steel buckling restrained brace · Behavior factor · Ductility factor · Non-linear time history analysis

1 Introduction

Braced frames are a very common form of construction, being economic to construct and simple to analyse. One of the major problems occurs in regular braces upon earthquake is the issue of member buckling. As a matter of fact, the bracing is gradually and permanently lengthened during earthquake and upon returning, such inelastic elongation results in bracing buckling and in further cycles, shows late resistance, which results in further energy absorption in irreplaceable members and joints of moment frame as well as more increase in structure displacement. During recent decades, buckling restrained brace (BRB) was used to overcome such problems of common bracings due to high ductility, symmetric hysteresis behavior and proper energy absorbability.

Wakabayashi et al. (1973) suggested a bracing system composed of a steel plate core surrounded by two pre-fabricated concrete wall panels. Kimura et al. (1976) presented another type of BRB, through placement of steel core in steel tube filled with cement mortar. Such type of brace is composed of a casing and a metal core. Mochizuki et al. (1979) suggested a series of tests on bracings using a layer of absorbing materials to prevent adhesiveness between steel core and concrete and such absorbing materials enable cross movement to steel core against compressive loads. Such type of BRBs are known as unbounded BRB. Steel core resists against axial force and bending stiffness of the external tube prevents core from buckling. In common specimens, the steel core is placed inside a metal casing filled with concrete mortar to prevent buckling under compression. Prior to filling the casing by concrete, some spacer material is placed between steel core and mortar to prevent transmission of axial force from steel core to concrete. Meanwhile, the effect of Poisson coefficient results in inflation of steel core under compression which requires provision of such gaps. In this system there is a need to provide a sliding surface or

✉ Mehdi Ebadi Jamkhaneh
mehdi.ebadi1985@hotmail.com; mehdi.ebadi@semnan.ac.ir

[1] Faculty of Civil Engineering, Semnan University, 19111-35131 Semnan, Iran

[2] School of Engineering, University of Birmingham, Birmingham, UK

[3] Urban Planning, Islamic Azad University, Science and Research Branch, Tehran, Iran

Published online: 05 January 2019

discontinuous layer between steel core and surrounding concrete. Concrete and external steel tube provide the needed stiffness and bending resistance to prevent global buckling of the brace and enable the steel core to bear load up to yielding without any loss of stiffness and resistance of bracing within loading cycles. Therefore, due to prevention of buckling, this system provides higher energy absorbability capability in comparison to common bracing systems. Wada et al. (1989) suggested that BRB may be designed and applied as a damper in dissipation of energy entering into the structure through a quake. Black et al. (2002) and Merritt et al. (2003) conducted low cycle fatigue tests to assess the behavior of BRBs. However, several weak points in BRB shall be solved. Such defects include complexity of contact boundary conditions between materials and components, time-consuming of manufacturing process and difficulty in detection of destruction level upon an earthquake.

All-steel BRBs, which do not require sliding materials or mortars, were introduced as a practicable solution to overcome the aforementioned problems of BRBs. Such braces are composed of a steel core and sheath, in which the buckling is controlled merely through making a gap between the core and sheath in one direction. Hoveidae and Rafezy (2012) examined the global buckling behavior of all-steel BRBs. The aim of study was conducting analytical studies on BRBs using a variety of gaps between core and external sheath. The results indicated that bending stiffness of BRB may significantly affect global buckling behavior. Hosseinzadeh and Mohebbi (2016) studied the behavior of all-steel BRB considering different gaps between core and steel casing. It was demonstrated through comparison of behavior of this bracing with regular convergent cross bracings that using all-steel BRBs may protect the structure within life safety level under seismic loads. Zhu et al. (2017) suggested the deformed type of BRB web to enable further resistance against out of plane buckling. This approach managed to show a good buckling strength against severe and high quake loads. Ebadi Jamkhaneh and Kafi (2018a, b), Ebadi Jamkhaneh et al. (2018a, b) and Ahadi koloo et al. (2018) offered a new type of all-steel BRBs, which provide the structure with high formability and energy absorbability in high deformations. They concluded that taking benefit from such type of bracings results in keeping the tall structure performance within the life safety level, unlike structures equipped with regular steel braces. Also, in case of buckling behavior of the plates, extensive studies were carried out by Mohammadzadeh and Noh (2014, 2015, 2016, 2017, 2018) and Mohammadzadeh et al. (2018).

From amongst the measures taken concerning prevention of core from buckling included using stiffener around steel core longitudinally to improve buckling resistance. Although utilizing these stiffeners increases construction costs and improves the buckling behavior of core plates to some extent, but brace resistance parameters will be controlled through the relevant components buckling. In this study, a new form of all-steel buckling restrained brace, which is different from previous specimens are introduced. The main reason of this study was to provide a model of the brace that does not require a welding process, and it is easy to use and erect. Therefore, here it is suggested corrugated steel plates which are inherently stiffened, instead of using smooth plates and welded stiffeners in braces. Meanwhile, thinner plates may also be used through applying this approach. Corrugated plates provide high out of plane stiffness due to their geometrical shape and shall have high buckling resistance against in-plane loads. Existence corrugates in the body of core, and tube enables a brace to bear high plastic deformations without the loss of resistance and also increases deformability and energy absorbability. Non-linear analysis of finite elements was conducted on specimens in order to study the seismic behavior of such type of system and compare the performance level with common braces. The behavior of this system is initially studied under cyclic loading and the seismic behavior of 4-, 8- and 12-story steel structures equipped with regular convergent cross bracings and the suggested bracing under non-linear static analysis are compared. The aim of the analysis is to compare the capacity of the two structures, the failure sequence, and their displacement behavior.

2 Finite Element Modeling of Proposed BRB

Numerical cyclic analysis was conducted on eight specimens using ABAQUSv6.14.2 (2014) software to study the behavior of proposed BRB. Three-dimensional (3D) models were applied in order to have a correct and better understanding on the behavior of this type of bracing. The models are composed of two steel sheaths with internal corrugated walls which are distant from each other merely from one direction.

Table 1 Properties of BRB specimens

No.	Model name	Internal tube thickness (mm)	External tube thickness (mm)	K_0 (kN/mm)
1	$B_{20}G_0$	8	10	384
2	$B_{20}G_5$	8	10	384
3	$B_{20}G_{10}$	8	10	384
4	$B_{20}G_{20}$	8	10	384
5	$B_{40}G_0$	10	12	768
6	$B_{40}G_5$	10	12	768
7	$B_{40}G_{10}$	10	12	768
8	$B_{40}G_{20}$	10	12	768

The details of these sections and sizes of proposed bracing numerical specimens have been given in Table 1.

Naming of the models is as follows: B represents distance between dents in mm and G represents distance between walls of two outer and inner sheaths in mm. Total specimens' length has been taken as 2000 mm. Static cycle analysis was carried out using ABAQUS/Standard program. All the bracing model members were meshed using S4R reduced integral first order elements. Considering the program regulations, the maximum and minimum increments were considered as 0.2 and 0.0001, respectively. Size of elements has been considered as 25 mm and 100 mm for the areas in vicinity to the force applying location and support and other parts, respectively. All the suggested bracing steel members were made from ST52 steel (yield strength: 370 MPa, Poisson coefficient: 0.3, Young modulus: 200 GPa).

A nonlinear isotropic-kinematic combined hardening rule was implemented to reproduce the plastic behavior of materials. The selection and calibration of steel material properties and hardening parameters were based on the results of a coupon test conducted by Tremblay et al. (2006). Accordingly, finite element (FE) results of this study were decided to be verified, based on those studies. The initial kinematic hardening modulus C and the rate factor γ were set to 8 GPa and 75, respectively. The material isotropic hardening parameters of the exponential law, Q_∞ and b, were chosen as 110 MPa and 4, respectively, according to Korzekwa and Tremblay (2009).

In Fig. 1a, b, the steel materials stress-strain curve resulted from monotonic and cyclic tests as well as cyclic response calibration has been given. Initially, the linear buckling analysis is done upon presence of a superficial load to the middle plate. The first buckling mode is considered for models geometrical imperfection. The boundary conditions in one ending of the bracing are hinge support and the axial displacement towards the other ending of the same enters into the end of the internal tube. Axial displacement applying to one side of the bracing is mentioned as follows as per the cyclic pseudo-static loading protocol, suggested by AISC regulations (2010) for BRBs: First of all, two cycles of $\pm\Delta_y$, two cycles of $\pm 0.5\Delta_{bm}$, two cycles of $\pm\Delta_{bm}$, two cycles of $\pm 1.5\Delta_{bm}$, and two final cycles of $\pm 2\Delta_{bm}$,Δ_y steel core yield displacement and Δ_{bm} bracing axial deformation in proportion to the story drift (2010).

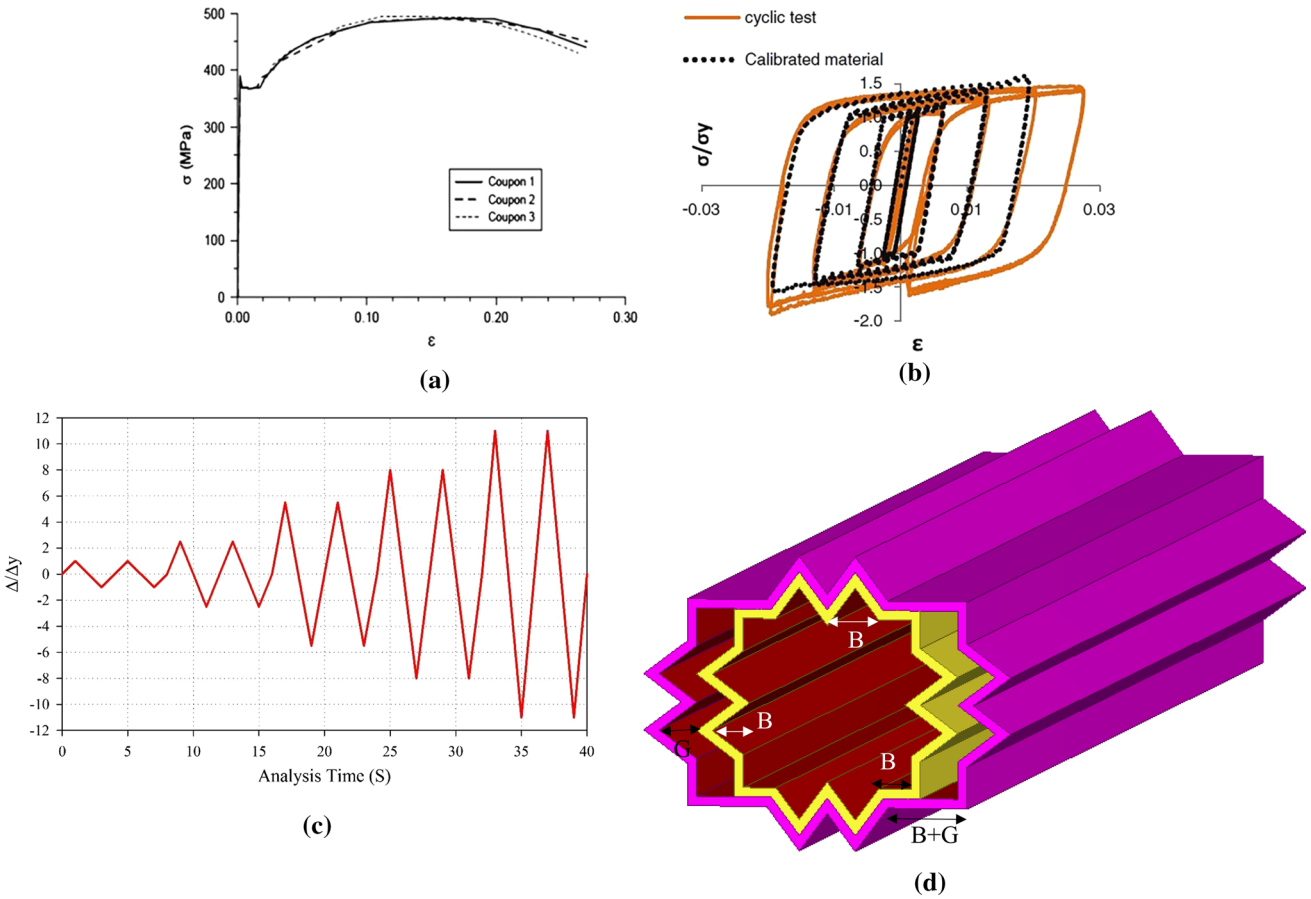

Fig. 1 **a** Monotonic experimental stress-strain curve; **b** cyclic experimental stress-strain curve and calibrated hysteretic response of the steel material; **c** loading protocol of the BRB models according to AISC seismic provisions and **d** proposed BRB

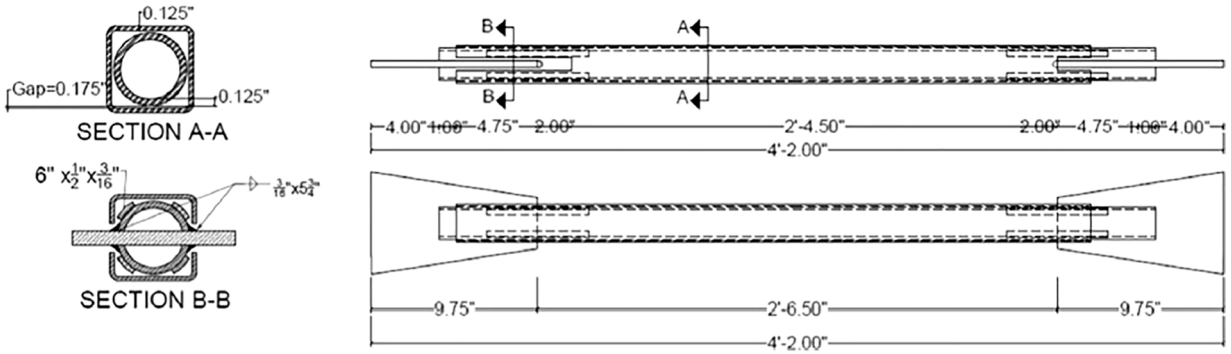

(a)

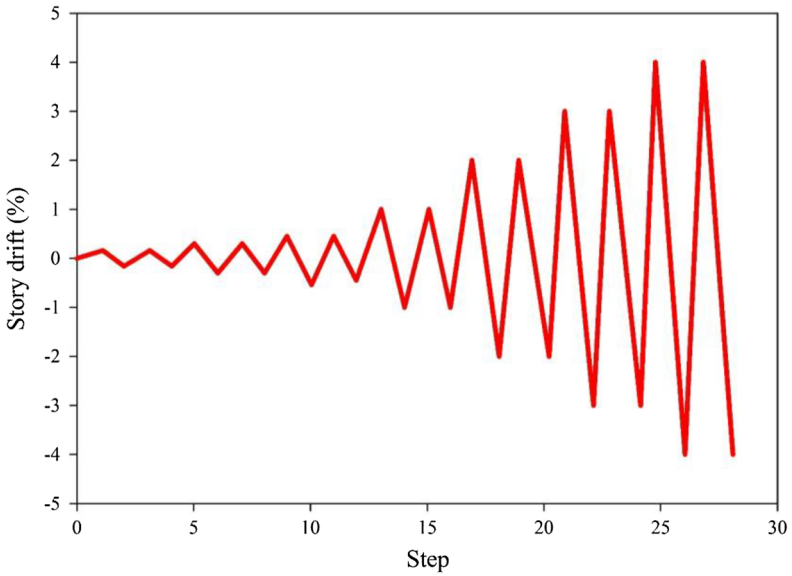

(b)

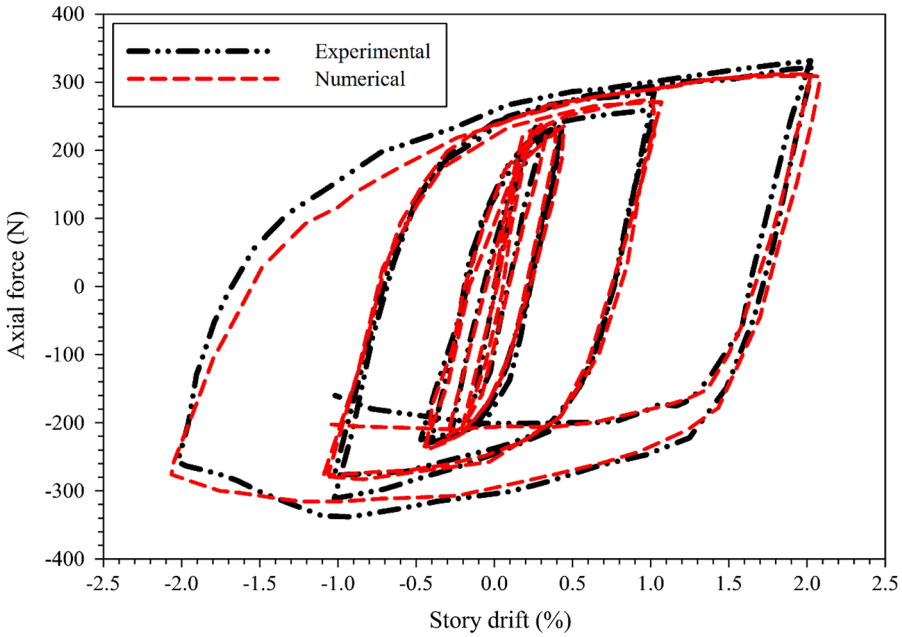

(c)

◂**Fig. 2** **a** Dimension and cross section of test specimens (Seker and Shen 2017); **b** loading protocol and **c** comparison of load-drift behaviors of the numerical model and the test specimens

Considering the previous conducted studies Trembley et al. (2006), the maximum strain throughout the bracing core for the common structural applications is between 0.01 and 0.02 and the maximum deformation in previous experimental studies was limited within the same range. In this study, Δ_{bm} was considered as 20 mm, which is in proportion to core axial 1% strain and Δ_y is equal to 3.7 mm. Therefore, the ultimate bracing axial displacement demand within transverse loading is roughly equal to 11 times Δ_y, representing steel core strain 2%. Figure 1c shows loading template. The proposed bracing meshed 3D section and elevation have been indicated in Fig. 1d.

2.1 Numerical Model Verification

In this section, proposed numerical model is validated by the results of the test specimen (Seker and Shen 2017). Brace sections are composed of two square-shaped sections, including the core of *HSS* 1.900×0.125, and *HSS* $2\,1/2 \times 2\,1/2 \times 1/8$ type for the external sheath. The opening gap between the two steel sections is 4.445 mm with a thickness of 3.2 mm. The total bracing length is equal to 1270 mm. The yield stresses of the core steel and external sheath are 289 MPa and 317 MPa, respectively. Figure 2a schematically shows the bracing cross section. Loading protocol was defined according to AISC regulations within the form of yield and designing displacements (Fig. 2b). In this study, the design drift was considered to be equal to 2% of floor height. The results of hysteresis behavior of the numerical model and experimental specimen (Seker and Shen 2017) have been demonstrated in Fig. 2c. As it is seen, like the experimental model, the behavior of the numerical model is sustainable up to the 8^{th} cycle and from the 9^{th} cycle, the strength of specimen decreases upon 1% of drift, which is due to bending deformation generated in the bracing joint end plate. Meanwhile, when the drift reaches 1.7% under compressive state, the plastic area is generated at external tube ending.

2.2 Finite Element Analysis Results

Hysteresis curve for all the 8 samples has been given in Fig. 3. As it is observed, samples with 10 mm and 20 mm gaps indicate signs of instability due to core plate buckling. Hysteresis curves envelope was extracted to use such bracing for strengthened frames inelastic analyses (Fig. 3c, d). As seen from the results of Fig. 3, size of bracing core does not significantly affect the sample nonlinear behavior.

3 Nonlinear Static Analysis

In the nonlinear static stage, a pushover analysis was conducted to assess the performance of the proposed all-steel BRBs. Initially, a study was conducted to compare the steel structures braced with X-bracings. Then, such cross bracings were replaced by BRBs, and the structure was strengthened and the analyses were repeated. In this study, three 4-, 8-, and 12-story structures were used to conduct the analyses. In Table 2, the particulars of the beam and column elements in the floors are presented. As shown, the height of each floor was considered to be 3.2 m. All three structures had a steel moment frame system, average formability with a special convergent bracing, and 15 m plan. Each structure included three spans, each 5 m in both directions, that are fully symmetric and regular in height and plan. Upon designing, the middle frame was selected and subjected to pushover analysis. These frames were primarily subjected to structural design and seismic loading in the SAP2000 v19.0.0 (2015) program according to AISC360-10 (2010) and the Building and Housing Resource Center (BHRC), Iranian Standard 2800 (2015), respectively. The beam-to-column connections were modeled in a fully rigid manner, and the value for the live load and for the dead load for all the ceilings was 4.5 and 2 kN/m^2, respectively (except for the roof, where it was equal to 1.5 kN/m^2). The column sections were of a box type and the beams were of beam plate type. The CX-Y expression is used to refer to columns, where C, X, and Y refer to the column, column exterior dimensions in millimeters, and column thickness in millimeters, respectively. Figure 4a–c shows the plan and frame with the bracing used before and after strengthening. Figure 4d, e shows the beam and bracing sections. Three frames of the 4-, 8-, and 12-story frames were subjected to pushover nonlinear static analysis in the SAP2000 v19.0.0 program with a 3.2 m height and three spans, each 5 m span. To strengthen the frames, the all-steel BRBs with similar shapes to that of the $B_{20}G_5$ specimen were replaced by cross-bracing specimens. The statuses of the plastic hinges in the targeted displacement are shown in Fig. 4f, g. The dimensionless push curve was used to model the BRBs according to the levels defined in FEMA 440 (2006) and is shown in Fig. 5a.

The performance level of the structure equipped with a convergent cross bracing was promoted from the collapse threshold to the life-safety area by replacing the common cross bracings in the 4-floor frame by the proposed bracing. For instance, for 8- and 12-story buildings, the total frame performance level was promoted to life safety. For

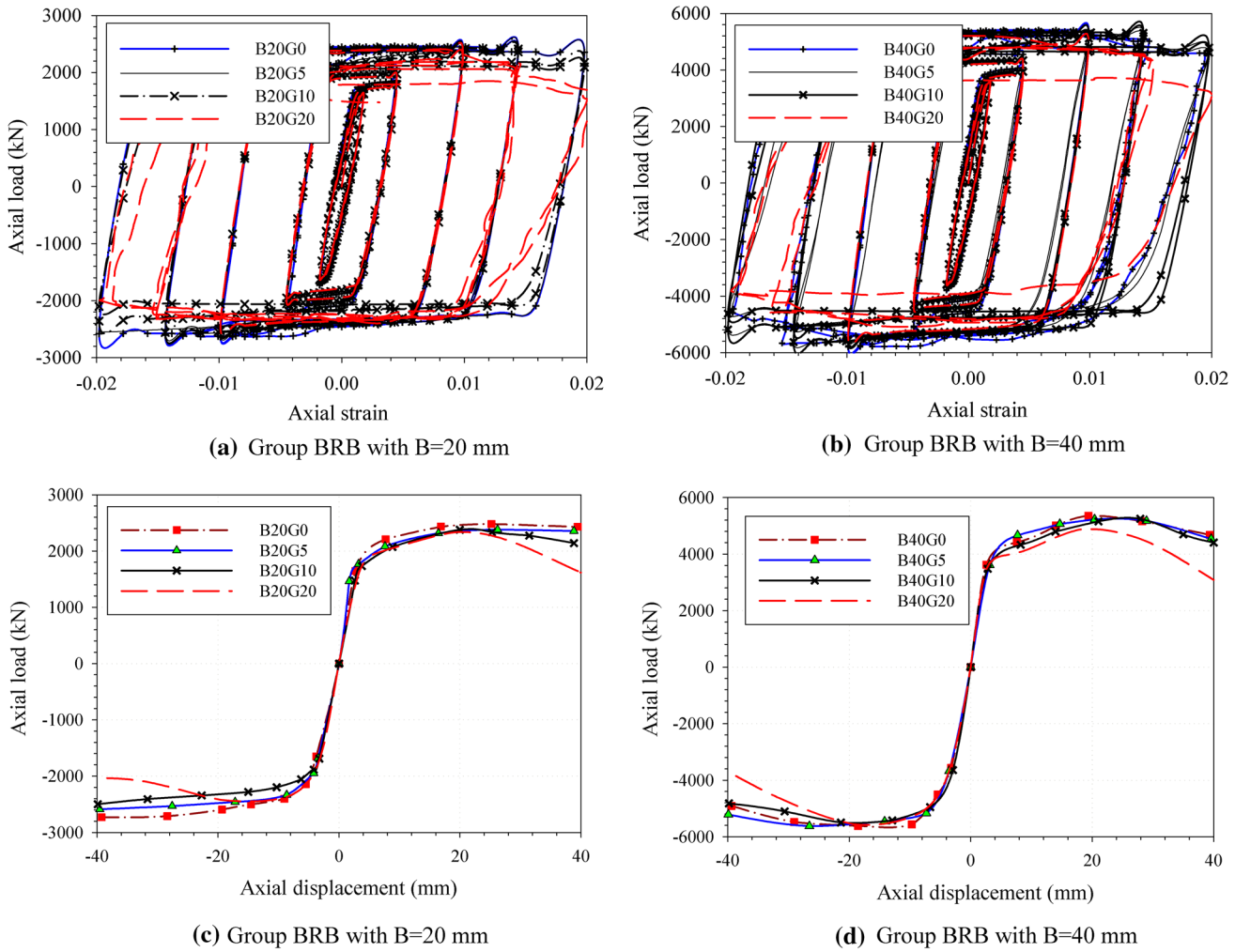

(a) Group BRB with B=20 mm

(b) Group BRB with B=40 mm

(c) Group BRB with B=20 mm

(d) Group BRB with B=40 mm

Fig. 3 Hysteretic curves of the proposed BRBs by group: **a** B = 20 mm; **b** B = 40 mm; **c** bilinear curves of the proposed BRBs by group B = 20 mm and **d** B = 40 mm

Table 2 Column, beam and brace dimensions (Unit: mm)

	Story level	Column	Beam $(b_f \times h_w \times t_f \times t_w)$	Brace $(b_b \times t_b)$
4-Story	1–2	C400-8	$110 \times 220 \times 10 \times 8$	80×8
	3–4	C350-8	$100 \times 200 \times 8 \times 6$	60×6
8-Story	1–2	C450-12	$140 \times 300 \times 12 \times 8$	120×12
	3–4	C450-10	$140 \times 300 \times 10 \times 8$	100×10
	5–6	C350-8	$120 \times 240 \times 10 \times 8$	80×8
	7–8	C300-8	$100 \times 200 \times 8 \times 6$	80×8
12-Story	1–3	C550-12	$170 \times 360 \times 12 \times 10$	160×14
	4–6	C500-12	$160 \times 340 \times 12 \times 10$	140×12
	7–8	C450-12	$150 \times 320 \times 12 \times 8$	120×12
	9–10	C350-12	$120 \times 260 \times 10 \times 8$	100×10
	11–12	C300-10	$100 \times 220 \times 10 \times 6$	80×8

the 1st-floor columns, the axial forces before and after strengthening of each of the three frames are presented in Tables 3 and 4. Average decreased axial force in first floor columns for 4-floor structure is roughly equal to 8%, while this is equal to 6% and 4% for 8-and 12-story structures, respectively.

In most cases, by decreasing the axial force value in the 1st- floor columns, the average axial force value fell below that of the compressive and tension capacities of the columns. Meanwhile, the maximum decrease was related to the short 4-story building with different frames. In Fig. 5b, the capacity curves of the frames resulting from the pushover analysis are shown for the frames with regular cross-convergent bracing and with BRBs. As seen from the curves in Fig. 5b, the presence of the suggested diagonal BRBs in the frames resulted in more ductile behavior than was found with regular cross-convergent bracing frames. The issue was the symmetric behavior of such types of bracing in tension

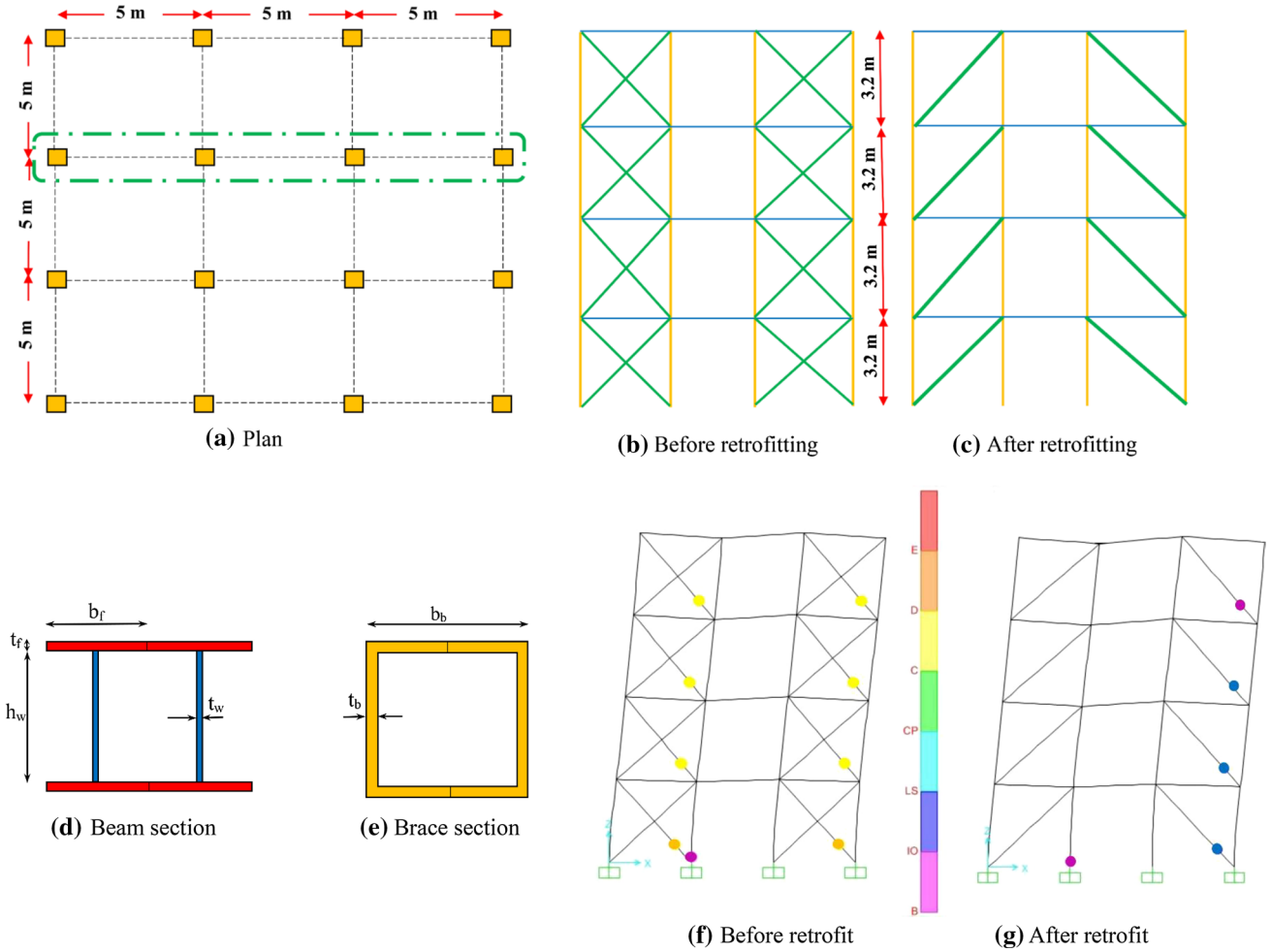

Fig. 4 Configuration of the 5-story braced frame before and after strengthening: **a** plan of the building; **b** before strengthening; **c** after retrofitting; **d** configuration of the beam sections; **e** brace section; **f** four-story frame before retrofit; **g** after retrofit

and compression. The area under the curves represents the absorption capacity of the specimens, which was significantly high in specimens with the suggested BRBs. In other words, failure of the structures equipped with the suggested BRB was delayed because of the suitable formability.

4 Calculation of the Behavior Coefficient for Structures

In the seismic design instructions for building structures, the most challenging part is associated with force reduction and deflection amplification factors. The force decrease coefficient was expressed as the structure-behavior-modification coefficient, R, from the Building Seismic Safety Council (BSSC) in the National Earthquake Hazards Reduction Program (NEHRP) (1998) recommendations (BSSC 1997) or as the system performance coefficient, R_w, from the Uniform Building Code of the International Conference of Building Officials (1988) and the Structural Engineers Association of California (SEAOC) (1988). The ductility coefficient is calculated, in Eq. (1), as follows:

$$\mu_s = \frac{\Delta_{\max}}{\Delta_y} \tag{1}$$

Considering the ductility result, the structure has a certain capacity for energy absorption and depreciation. Because of the same energy absorption among structures, the elastic design force, C_y, may be decreased to the yield strength level using the R_μ coefficient as follows:

$$R_\mu = \frac{C_{eu}}{C_y} \tag{2}$$

The important point is that the yield strength level refers to structure failure level and not to the first yield level. The viscose damping ratio was considered as 5% for calculating

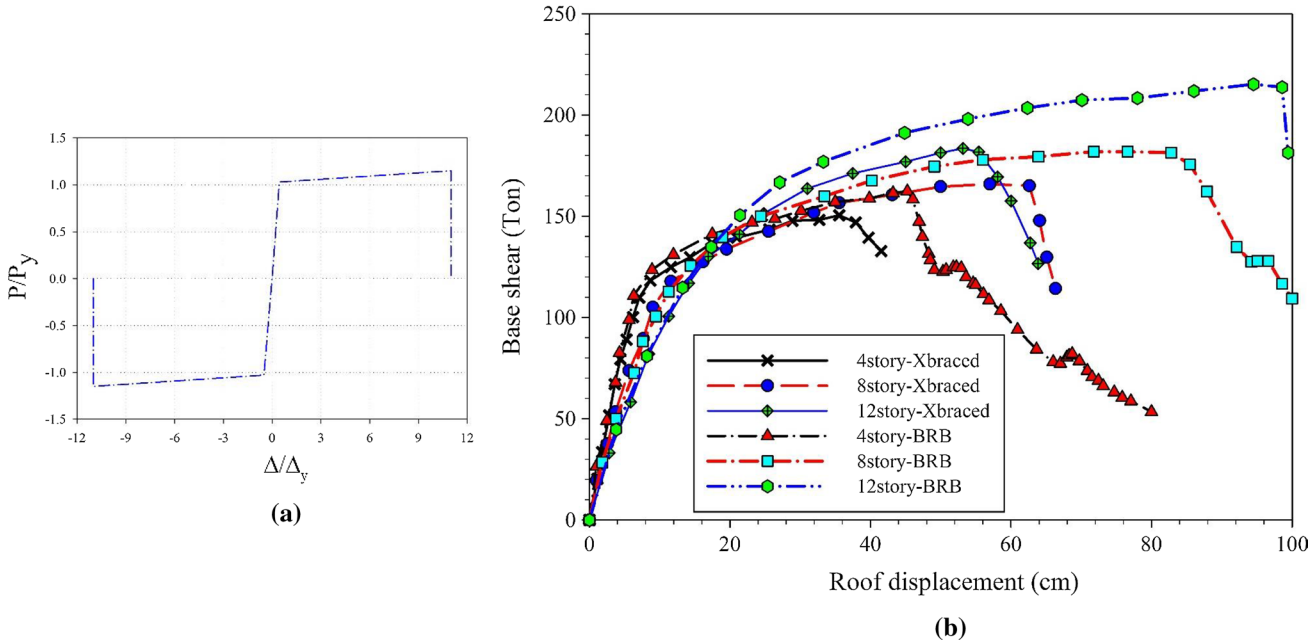

Fig. 5 **a** Modeling parameters and acceptance criteria of BRB specimens and **b** pushover curve of frames

Table 3 Determination of axial forces capacity

No. story	Section	Cross sectional area (cm^2)	λ (slenderness factor)	Length of element (cm)	Radius of gyration (cm)	F_a (Allowable stress) (kg/cm^2)	Compressive capacity (kg)	Tensional capacity (kg)
4	C400-8	125.44	19.98	320	16.01	1381.14	294,525	360,360
8	C500-15	291	16.15	320	19.81	1394.55	689,884	844,093
12	C550-15	321	14.65	320	21.85	1399.13	763,505	934,171

Table 4 Axial force values of the first level columns in X-braced and retrofitted frames

No. story	Column label	X-braced frame	Retrofitted frame	Reduction in axial force (%)
4	A	259.5	229.2	11.7
	B	280.1	259.5	7.4
	C	297.2	255.7	14
	D	246.8	243.2	1.5
8	A	565.8	514.4	9.1
	B	689.3	633	8.2
	C	604.2	592.5	1.9
	D	519.1	502.2	3.3
12	A	659	632.7	4
	B	711.6	691.7	2.8
	C	769.4	728.4	5.3
	D	646.7	619.8	4.2

such a decreased coefficient caused by ductility. For a system with one degree of freedom (DOF), the formula for determining the difference between the ductility and the decreased ductility coefficients comes from the formulas presented by Newmark and Hall (1982) and Riddell et al.

(1989). The remaining strength between the real structure yield level, C_y, and first effective yield level, C_s from the NEHRP regulations (BSSC 1997) are defined as the following overstrength coefficient:

$$\Omega = \frac{C_y}{C_s} = \frac{\Delta_y}{\Delta_s} \tag{3}$$

This over-strength of a structure resulted from the internal force distribution caused by the strength of the materials being greater than was considered in the design, including strain hardening, added section dimensions, combinations of different loadings, and effects of nonstructural elements, and the like. The allowable stress coefficient was considered for the difference in materials by law. For designing an allowable stress method, the design force level. C_w, was decreased from the initial yield surface, C_s, with the Y coefficient as follows:

$$C_w = \frac{C_s}{Y} \tag{4}$$

The Y value fell between 1.4 and 1.5. Eventually, the behavior coefficient in designing was calculated using the allowable stress method as follows in Eq. (5):

$$R = \frac{C_{eu}}{C_W} = \left(\frac{C_{eu}}{C_y}\right) \times \left(\frac{C_y}{C_S}\right) \times \left(\frac{C_s}{C_w}\right) = R_\mu \times \Omega \times Y \tag{5}$$

Meanwhile, the deflection amplification coefficient, C_d, which is the ratio between Δ_{max} and Δ_s, may be calculated using Eq. (6) as

$$C_d = \mu_s \times \Omega \tag{6}$$

In Table 5, the overstrength, ductility, and behavior coefficients and the deflection amplification factors for the frames, before and after strengthening, are presented. Considering the results, the structural response modification coefficient with the proposed BRB was bigger than the frame system with regular cross convergent bracing because the BRBs had a higher ductility coefficient. Meanwhile, from the results, it was inferred that upon increasing the structure height, the structure behavior coefficient decreased.

Table 5 The response modification factor of all-steel BRBs and X-braced frames

No. story	Type of frame	Ω	R_μ	R	C_d
4	Proposed BRB	1.63	5.27	12.03	6.81
8	Proposed BRB	1.62	4.77	10.82	6.42
12	Proposed BRB	1.58	3.85	8.52	5.23
4	X-bracing	1.51	4.33	9.15	4.33
8	X-bracing	1.48	3.96	8.20	3.87
12	X-bracing	1.42	3.16	6.24	3.64

5 Nonlinear Time History Analysis

Finally, the nonlinear time-history analysis was carried out for two states of frames before and after strengthening, and the results took the form of the distribution floor drift ratio for each accelerogram. The particulars of the two accelerograms of the near field and two accelerograms of the far field are listed in Table 6 with respect to FEMA P695 suggestions (2009). In Fig. 6, a comparison is shown between the floor drift ratios in all the models without and with strengthening in quakes of both near and far fields. Considering the results, the floor drift ratio for the strengthened frames was a little

Table 6 Earthquake data for the parametric analysis

Earthquake motion parameters	Northridge (USA)	Kobe (Japan)	El-Centro (USA)	Hachinohe(Japan)
Date of occurrence	1994	1995	1940	1968
Magnitude of earthquake, M_w	6.7	6.8	6.9	7.5
Maximum horizontal acceleration, (g)	0.843	0.834	0.349	0.231
Predominant period, T_p (sec)	0.36	0.36	0.56	0.22
Significant duration, D_{5-95} (sec)	5.32	8.4	24.58	27.79
Time of MHA (t_p (sec))	4.2	8.52	4.1	4.18
PGV/PGA (s)	0.157	0.112	0.102	0.146
Arias intensity (m/s)	5.004	8.389	1.758	0.899
SIR (m/s/s)	1.903	1.407	0.117	0.037
Energy flux (J m^{-2} s^{-1})	8560.187	7649.179	2144.177	2409.691
Type	Near field	Near field	Far field	Far field
Hypocentral distance (km)	9.2	7.4	15.69	14.1

$SIR = I_{a(5-75)}/D_{(5-75)}$

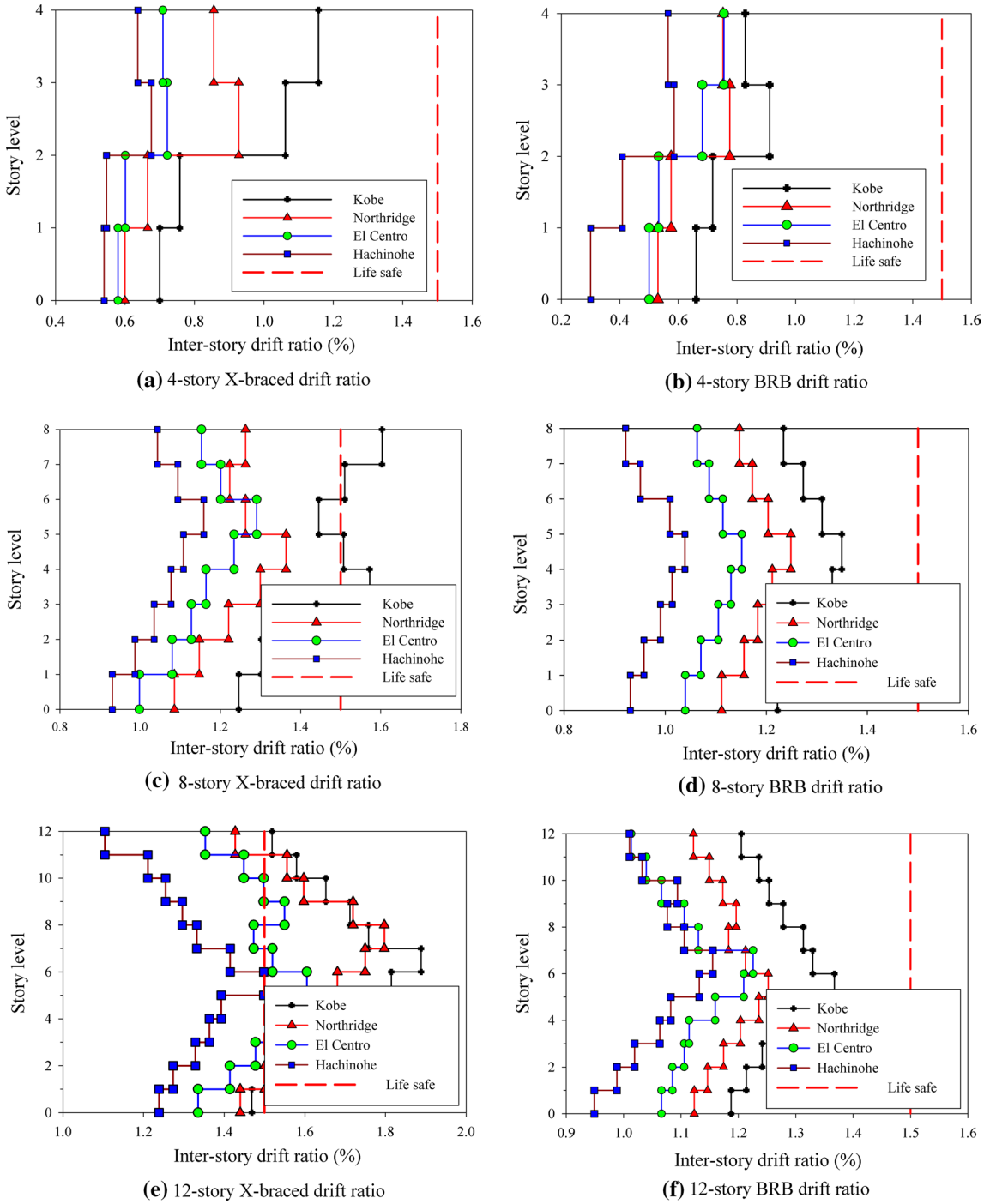

Fig. 6 Inter-story drift ratio of structures: **a** 4-story X-braced drift ratio; **b** 4-story BRB-braced drift ratio; **c** 8-story X-braced drift ratio; **d** 8-story BRB-braced drift ratio; **e** 12-story X-braced drift ratio; **f** 12-story BRB-braced drift ratio

less than it was for the frames with regular cross-convergent bracing. The symmetric behavior of the cross-convergent bracings may be an acceptable explanation for this difference; that is, the regular bracings were subjected to strength loss and yield after a couple of cycles because of buckling problems.

Performance levels were used to describe the state of the structures after being subjected to a certain hazard level, and those based on FEMA 273 (1997) were classified as fully operational, operational, life safe, near collapse, and collapse. Overall lateral deflection, ductility demand, and inter-story drifts were the most commonly used damage

parameters. Each of the five qualitative levels was related to a corresponding quantitative maximum inter-story drift (as a damage parameter) as follows: $<0.2\%$, $<0.5\%$, $<1.5\%$, $<2.5\%$, and $>2.5\%$, respectively.

The floor drift ratio charts show that the regular bracings in a 4- story low building managed to keep the structure within the life-safety region under both the near-field and far-field types of time histories. However, when the number of floors was increased from 4 to 8, it was seen that the structure with the regular cross-convergent bracings shown in the accelerogram for the near field of Kobe failed to remain in the life-safety region. By replacing the X bracings with the suggested BRBs, the structure performance level was kept in the life-safety region. For those of a 12-story frame, the structure was at collapse in all the near-field and far-field accelerograms, while the structure performance level to the life-safety level was changed through strengthening. Considering these results, it can be inferred that the maximum story drift ratio was generated with the near-field accelerogram, and that such an effect was seen more often in tall structures.

6 Conclusion

The new all steel buckling-restrained brace introduced in this study is composed of two tubes with corrugated walls inside each other. The existence of these triangular dents on the surface of tube results in inherent increase of resistance against buckling, through which in addition to prevention of pre-mature failure of the relevant member, energy absorption is also improved significantly in the system. Whereas stiffness and resistance are two deterministic factors in systems resisting against lateral loads, here initially through changing parameters of gap between two tubes and dimensions of the brace section, several cyclic analyses were conducted in ABAQUS finite element program to enable determining non-linear modeling parameters. Then, the performances of 4-, 8- and 12-story frames equipped with suggested BRB have been examined and assessed using SAP program and through conducting pushover analyses and non-linear time history. In the following the brief of analyses findings are presented:

1. Taking benefit from suggested all steel buckling-resistant braces for strengthening 4-, 8- and 12-story frames results in maintenance of structure performance level within life-safety zone in pushover analyses. This is while in frames with regular convergent crossed bracing in 8- and 12-story frames structure global performance has entered into failure zone.
2. The axial forces imposed to columns of first floor of a strengthened 4-story frame have managed to achieve 8% decrease in comparison to frame without strengthening. Such value has reached to 6% and 4% for 8- and 12-story structures, respectively. Due to stiffness in strengthening steel structure, it seems that using of all-steel BRB and reducing sizes thereof may be a good to explanation for using of these braces.
3. The behavior and ductility factors for all-steel BRBs are roughly bigger than frames with a regular crossed braced for 22% and 30%, respectively. Evidently, taller frames have lower ductility and behavior factors.
4. Average of the maximum value of inter-story drift ratio for 4-, 8- and 12-story retrofitted frames shows a decrease of 4%, 11% and 23% decrease under far field earthquakes, respectively. A frame with taller height (12-story) has not managed to remain within life safety zone while this case was addressed using suggested all steel buckling resistant braces.
5. The average decrease of inter-story drift for strengthened 4-, 8- and 12-story frames with respect to frame with regular crossed convergent brace are equal to 19%, 12% and 29%, respectively, under near field quakes. Unlike far field, in the 8-story frame under Kobe earthquake, crossed bracing frame performance level exited from life safety zone and in the 12-story frame, it entered into collapse prevention state under both accelerograms. Utilizing of the suggested diagonal braces has resulted in an increase in performance level and change it to the life safety performance level.
6. According to the present research, it is suggested to conduct experimental studies on the proposed specimens and incremental dynamic analysis (IDA) on the frames equipped with these braces.

References

ABAQUS Standard User's Manual The Abaqus Software is a product of Dassault Systèmes Simulia Corp., Providence, RI, USA Dassault Systèmes, Version 6.14.2, USA, 2014.

Ahadi Koloo, F., Badakhshan, A., Fallahnejad, H., Ebadi Jamkhaneh, M., & Ahmadi, M. (2018). Investigation of proposed concrete filled steel tube connections under reversed cyclic loading. *International Journal of Steel Structures, 18*(1), 163–177.

AISC (American Institute of Steel Construction). (2010). *Specification for structural steel buildings. ANSI/AISC 360-10*. Chicago, IL: American Institute of Steel Construction.

BHRC. (2015). Iranian national building code, Tehran.

BSSC. (1997). NEHRP Recommended provisions for seismic regulations for new buildings andother structures, 1997 edition, Part 1: Provisions and Part 2: Commentary, prepared by the building seismicsafety council for the federal emergency management agency (Report Nos. FEMA 302 and 303),Washington, D.C.

Black, C., Makris, N., & Aiken, I. (2002). Component testing, stability analysis and characterization of buckling restrained braces. *PEER*

report 2002/08. Pacific Earthquake Engineering Research Center, University of California at Berkeley.

Ebadi Jamkhaneh, M., Homaioon Ebrahimi, A., & Shokri Amiri, M. (2018a). Seismic performance of steel-braced frames with an all-steel buckling restrained brace. *Practice Periodical on Structural Design and Construction, 23*(3), 04018016.

Ebadi Jamkhaneh, M., Homaioon Ebrahimi, A., & Shokri Amiri, M. (2018b). Experimental and numerical investigation of steel moment resisting frame with U-shaped metallic yielding damper. *International Journal of Steel Structures*. https://doi.org/10.1007/s13296-018-0166-z.

Ebadi Jamkhaneh, M., & Kafi, M. A. (2018a). Equalizing octagonal PEC columns with steel columns: Experimental and theoretical study. *Practice Periodical on Structural Design and Construction, 23*(3), 04018012.

Ebadi Jamkhaneh, M., & Kafi, M. A. (2018b). Experimental and numerical study of octagonal composite column subject to various loading. *Periodica Polytechnica Civil Engineering, 62*(2), 413–422.

FEMA (Federal Emergency Management Agency). (2006). FEMA-440, Washington, DC.

FEMA (Federal Emergency Management Agency). (2009). FEMA-P695, Washington, DC.

FEMA 273. (1997). *NEHRP guidelines for the seismic rehabilitation of buildings, prepared by the Applied Technology Council for FEMA*. Washington, DC: Federal Emergency Management Agency.

Hosseinzadeh, S. H., & Mohebi, B. (2016). Seismic evaluation of all-steel buckling restrained braces using finite element analysis. *Journal of Constructional Steel Research, 119,* 76–84.

Hoveidae, N., & Rafezy, B. (2012). Overall buckling behavior of all-steel buckling restrained braces. *Journal of Constructional Steel Research, 79*, 151–158.

Kimura, K., Yoshizaki, K., & Takeda, T. (1976). Tests on braces encased by mortar infilled steel tubes. *Summaries of technical papers of annual meeting* (pp. 1041–1042).

Korzekwa, A., & Tremblay, R. (2009). Numerical simulation of the cyclic inelastic behavior of buckling restrained braces. In *International specialty conference on behavior of steel structures in seismic area* (*STESSA*), Montreal, Canada.

Merritt, S., Uang, C. M., & Benzoni, G. (2003). Sub-assemblage testing of core-brace buckling-restrained braces. *Report No. TR-2003/01*. University of California, San Diego, USA.

Mochizuki, S., Murata, Y., Andou, N., & Takahashi, S. (1979). *Experimental study on buckling of unbonded braces under axial forces: Parts 1 and 2* (pp. 1623–1626)., Summaries of technical papers of annual meeting Tokyo: Architectural Institute of Japan.

Mohammadzadeh, B., Choi, E., & Kim, W. J. (2018). Comprehensive investigation of buckling behavior of plates considering effects of holes. *Structural Engineering and Mechanics, 68*(2), 261–275.

Mohammadzadeh, B., & Noh, H. C. (2014). Use of buckling coefficient in predicting buckling load of plates with and without holes. *Journal of Korean Society for Advanced Composite Structures, 5*(3), 1–7.

Mohammadzadeh, B., & Noh, H. C. (2015). Numerical analysis of dynamic responses of the plate subjected to impulsive loads. *International Journal of Civil, Environmental, Structural, Construction and Architectural Engineering, 9*(9), 1194–1197.

Mohammadzadeh, B., & Noh, H. C. (2016). Investigation into buckling coefficients of plates with holes considering variation of hole size and plate thickness. *Mechanika, 22*(3), 167–175.

Mohammadzadeh, B., & Noh, H. C. (2017). Analytical method to investigate nonlinear dynamic responses of sandwich plates with FGM faces resting on elastic foundation considering blast loads. *Composite Structures, 174,* 142–157.

Mohammadzadeh, B., & Noh, H. C. (2018). An analytical and numerical investigation on the dynamic responses of steel plates considering the blast loads. *International Journal of Steel Structures*. https://doi.org/10.1007/s13296-018-0150-7.

NEHRP. (1998). *Recommended provisions for the development of seismic regulations for new buildings*. Washington, DC: Building Seismic Safety Council.

Newmark, N. M., & Hall, W. J. (1982). *Earthquake spectra and design*. El Cerrito, CA: Earthquake Engineering Research Institute.

Riddell, R., Hidalgo, P., & Cruz, E. (1989). Response modification factors for earthquake resistant design of short period buildings. *Earthquake Spectra, 5*(3), 571–590.

SAP2000®Version 19. (2015). *Linear and nonlinear static and dynamic analysis and design of three dimensional structures*. Berkeley, CA: Computers and Structures Inc.

SEAOC Structural Engineers Association of California. (1988). *Recommended lateral force requirements and tentative commentary*. San Francisco, CA: Seismological Committee, Structural Engineers Association of California.

Seker, O., & Shen, J. (2017). Developing an all-steel buckling controlled brace. *Journal of Constructional Steel Research, 131,* 94–109.

Tremblay, R., Bolduc, P., Neville, R., & Devall, R. (2006). Seismic testing and performance of buckling-restrained bracing systems. *Canadian Journal of Civil Engineering, 32*(2), 183–198.

UBC (Uniform Building Code). (1988). Int. Conf. of Bldg. Officials, Whittier, CA.

Wada, A., Saeki, E., Takeuchi, T., & Watanabe, A. (1989). *Development of unbonded brace, column* (Vol. 115). Tokyo: Nippon Steel Publication.

Wakabayashi, M., Nakamura, T., Katagihara, A., Yogoyama, H., & Morisono, T. (1973). Experimental study on the elastoplastic behavior of braces enclosed by precast concrete panels under horizontal cyclic loading—Parts 1 and 2. *Summaries of Technical Papers of Annual Meeting, 6,* 121–128.

Zhu, B. L., Guo, Y. L., Zhou, P., Bradford, M. A., & Pi, Y. L. (2017). Numerical and experimental studies of corrugated-web-connected buckling-restrained braces. *Engineering Structures, 134,* 107–124.